Improving Accuracy of Intravoxel Incoherent Motion Reconstruction using Kalman Filter in Combination with Neural Networks: A Simulation Study

Sam Sharifzadeh Javidi (PhD Candidate)[1,2], Reza Ahadi (PhD)[3], Hamidreza Saligheh Rad (PhD)[1,2]*

[1]Department of Physics and Medical Engineering, Medicine School, Tehran University of Medical Sciences, Tehran, Iran
[2]Quantitative Medical Imaging Systems Group, Research Center for Molecular and Cellular Imaging, Tehran University of Medical Sciences, Tehran, Iran
[3]Department of Anatomy, Medicine School, Iran University of Medical Sciences, Tehran, Iran

ABSTRACT

Background: The intravoxel Incoherent Motion (IVIM) model extracts perfusion map and diffusion coefficient map using diffusion-weighted imaging. The main limitation of this model is inaccuracy in the presence of noise.

Objective: This study aims to improve the accuracy of IVIM output parameters.

Material and Methods: In this simulated and analytical study, the Kalman filter is applied to reject artifact and measurement noise. The proposed method purifies the diffusion coefficient from blood motion and noise, and then an artificial neural network is deployed in estimating perfusion parameters.

Results: Based on the T-test results, however, the estimated parameters of the conventional method were significantly different from actual values, those of the proposed method were not substantially different from actual. The accuracy of f and D^* also was improved by using Artificial Neural Network (ANN) and their bias was minimized to 4% and 12%, respectively.

Conclusion: The proposed method outperforms the conventional method and is a promising technique, leading to reproducible and valid maps of D, f, and D^*.

Citation: Sharifzadeh Javidi S, Ahadi R, Saligheh Rad H. Improving Accuracy of In-travoxel Incoherent Motion Reconstruction using Kalman Filter in Combination with Neural Networks: A Simulation Study. *J Biomed Phys Eng*. 2024;14(2):141-150. doi: 10.31661/jbpe.v0i0.2104-1313.

Keyword

Intravoxel Incoherent Motion; IVIM; Perfusion Imaging; Diffusion Magnetic Resonance Imaging; Kalman Filter; Neural Networks, Computer

Introduction

Diffusion-weighted magnetic resonance imaging (DWI) uses motion-sensitive gradients to trace self-diffusion of water molecules in tissues, which has some derivations such as diffusion tensor imaging (DTI) [1] and intravoxel incoherent motion (IVIM) [2, 3]. DWI sequences are being applied in many radiological examinations to diagnose diseases and assess therapeutic procedures [4-9]. The signal decay of DWI depends on the random fluctuations of water molecules within voxels [10]. Extracellular water molecules move freely compared to intracellular water molecules that are highly curbed in their displacements because of the presence of macromolecules, cell membranes, and intracellular organelles. Diffusion-Weighted-Magnetic Resonance Imaging (DW-MRI) sequences can measure the self-

*Corresponding author: Hamidreza Saligheh Rad Quantitative Medical Imaging Systems Group, Research Center for Molecular and Cellular Imaging, Emam Khomeini Hospital, Keshavarz Boulevard, Tehran, Iran
E-mail: hamid.saligheh@gmail.com

Received: 20 April 2021
Accepted: 16 June 2021

diffusion of water in tissues as a factor of tissue cellularity at each voxel. High cellularity tissues delimit water molecules motion more than regions such as necrosis in which cell density is reduced because of hurts or injuries.

Random displacements of water molecules at body temperature are around 30 um in free space at about 50 ms. Although tissue cells and their substructures are in this size range and prevent water molecules movement. Thus, water movements in different tissues are not the same; accordingly, MR images can be sensitized to water molecules' displacements by diffusion sensitizing gradients and measures signal decay related to water diffusivity [11, 12]. Both gradient magnitude and diffusion time (duration of gradient operation) are essential in measuring signal intensity losses and making a factor so-called b-value, i.e. no motion in a voxel, no signal decays. However, motion can dramatically cause a signal loss and its ratio is proportional to the b-value. In other words, when the b-value is zero (b=0), non-restricted water (like CSF) is bright in the image. At lower b-values (smaller than 200), significant movements such as blood motions are gradually vanishing. Finally, water molecule movements disappear at higher b-values, then just dense tissues or malignant tumors are bright in images [13-15].

Based on blood circulation, water displacements are much greater than that of self-diffusion such that for increased b-values, perfusion signal decay approaches near zero. D using higher b-values is calculated (greater than 200 (mm^2)/sec), and f and D^* are also computed at lower b-values (smaller than 200 (mm^2)/sec). In a nutshell, DWI imaging employs functional information (f and D^* maps) as well as structural information (D maps) that could be deployed in the differentiation of normal and diseased tissues.

In most clinical studies, only the apparent diffusion coefficient (ADC) was reported; thus, it is not possible to deploy perfusion information that can enrich diagnosis [16]. The interpretation of clinical DWI images is important in this approach since lesion identification is based on ADC with both perfusion and diffusion characteristics mixed in itself [17]. Some limitations, such as long acquisition time and inaccuracy of IVIM parameters, restrict IVIM applications in clinical settings [3].

Single-shot echo-planar imaging (SS-EPI) techniques are used for imaging time and patient movement artifacts during DWI, offering significantly faster imaging [13]. Since noise and the portion of perfusion signal decay is in the range of noise level, the output parameters of IVIM are sometimes disturbed and inaccurate [6]. Several solutions have been presented such as the segmented method, Bayesian distribution, and dictionary-based [18-22]; however, their results are not highly accurate. In this study, a two-step method was proposed to decrease these limitations: 1) using the Kalman filter, the bias of the diffusion coefficient was minimized and 2) D^* and f were calculated by neural networks.

Material and Methods

This is an analytical and simulation-based research. Following is a description of the IVIM model and our method.

IVIM

Le Bihan introduced the IVIM model in 1986 [2, 23] and formulated IVIM models as follows equation (1):

$$S_b = fS_0 e^{-bD^*} + (1-f)S_0 e^{-bD} \quad (1)$$

where S_b and S_0 are signal intensities with and without b-values; D, f, and D^* are diffusion coefficient, blood, and pseudo-diffusion coefficient, respectively. Due to another source of motion, blood motion, in living tissues compared to non-living objects, it is predictable that the behavior of signal intensity decay would be bi-exponential in living tissues. The first exponent is because of blood motion and self-diffusion of water causes a

second exponent.

Simulations

This research aims to improve the IVIM parameters' reproducibility by employing the Kalman filter and neural networks. To the best of our knowledge, the most common method for IVIM parameters is a two-step or segmented approach, presuming perfusion parameters for higher b-values (b>200) that were close to zero. Then D is calculated in the first step using high b-values. To calculate f and D^* based on the estimated D and lower b-values (b<200) intensities, in the second step, a curve fitting algorithm like Levenberg–Marquardt algorithm was used. However, these methods calculate parameters, their outputs are not entirely accurate because they eliminate the effects of the perfusion parameter in the first step, showing its impact with a bias. The second step also suffers from noise and also nonlinear-model fittings depend on initial values and boundary conditions; therefore, the IVIM results tend to approach boundary conditions.

A combination of the Kalman filter and artificial neural network was proposed to overcome these limitations. Since some parameters were to be initialized, all of the needed parameters were calculated using an ANN. After that, to reduce D's bias using the Kalman filter, the perfusion effects were considered as a variable input that decreases with increasing b-value. Finally, a neural network was implemented for nonlinearity and noise in the second step.

The proposed method is applied to estimate IVIM parameters in a Monte-Carlo simulation. First, IVIM signal intensities were generated using Equation (1) and contaminated by additive complex Gaussian noise such that SNR=100, which was in the range of routine DW imaging. IVIM output parameters were calculated using the proposed method by 100,000 times. Finally, results and ground truth were compared, and bias and correlation of each parameter were calculated. Two setups were considered: 1) checking the accuracy of the Kalman filter in estimating true D and 2) examining the validity of all parameters in a realistic range of possible physiologic. In the first experience, parameters were constant D=0.001, f=0.1, and D^*=0.01. However, on the other setup, a complete range of possible physiologic data was considered and outputs were the result of the combination of Kalman filter and neural network. In the second experience, D, f, and D^* were in the range of [0.0003-0.0021], [0.02-0.34], and [0.009-0.034], respectively. The process of the proposed method is depicted on a flowchart (see Figure 1a).

Kalman Filter

The Kalman filter is a recursive method for minimizing the error of the estimation optimally [24] and applying widely in navigation systems and the field of machine vision to estimate the state of a dynamic system from the noisy measurement [25]. The Kalman filter is also an appropriate approach for estimating the DWI image parameters when the new DWI measurements are used to modify the previous amount. Since the Kalman filter is formulated based on a state-space model, the problem should be redefined in state space and this filter predicts the value based on the system and updates the predicted values based on new observations. The initial guesses of parameters are set to the results of ANN.

In methods such as the segmented method, perfusion decay at high b-values almost equals zero; then the IVIM model is converted to one compartment diffusion model by Stejskal-Tanner [10] so that the diffusion coefficient is easily calculable by Equation 2, 3.

$$S_b = \overbrace{fS_0 e^{-bD^*}}^{\alpha=0} + (1-f)S_0 e^{-bD} \tag{2}$$

$$\frac{S_{b_2}}{S_{b_1}} = \frac{(1-f)S_0 e^{-b_2 D}}{(1-f)S_0 e^{-b_1 D}} = e^{(b_1-b_2)D} \tag{3}$$

In the proposed method, the effect of perfusion decay on the contrary with other methods,

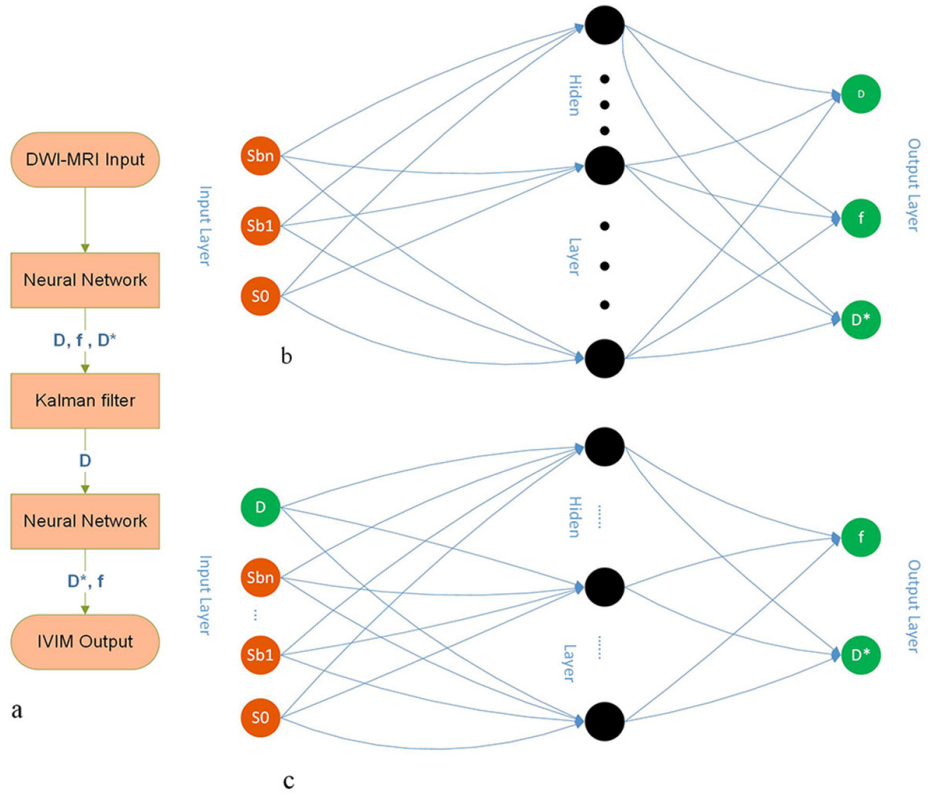

Figure 1: a) Flowchart of proposed method **b**) neural networks that estimated all of the output parameters **c**) estimated diffusion coefficient, which is the result of the Kalman filter, fed into the neural network and perfusion parameters are estimated by neural network

almost equal to zero, is considered.

$$\frac{S_{b_2}-\alpha_2}{S_{b_1}-\alpha_1}=\frac{S_{b_2}\beta_2}{S_{b_1}\beta_1}=\gamma\frac{S_{b_2}}{S_{b_1}}=\frac{(1-f)S_0e^{-b_2D}}{(1-f)S_0e^{-b_1D}}=e^{(b_1-b_2)D} \quad (4)$$

$$\ln\gamma+\ln\frac{S_{b_2}}{S_{b_1}}=(b_1-b_2)D \quad (5)$$

$$\frac{\overbrace{\ln\gamma}^{-u}}{b_1-b_2}+\frac{\overbrace{\ln\frac{S_{b_2}}{S_{b_1}}}^{y}}{b_1-b_2}=\overbrace{D}^{x} \quad (6)$$

$$\begin{aligned} x &= x \\ y &= x + u \end{aligned} \quad (7)$$

Where b_1 and b_2 are low and high b-values, Sb_1 and Sb_2 are signal intensities for b_1 and b_2, respectively. α is a perfusion portion of the signal, β is (1-α)/S and γ is the β_2/β_1. After some simplifications described in Equations (4, 5, 6), finally, Equation (7) is used in the Kalman filter, where u is the input related to perfusion decay.

Neural Networks

In this work, two feed-forward neural networks with the default setting of one hidden layer were implemented using the Neural Network Toolbox provided by Matlab (Version: R2018a, The Mathworks Inc., Natick, MA, USA). The first ANN is composed of the input layer, including 14 inputs representing the DWI signal intensity for each b-value, one hidden layer with 14 nodes and the output layer illustrated the amounts of D, f, and D* (Figure 1b) feeding the Kalman filter. The second ANN is composed of the input layer, including 15 inputs representing the DWI signal intensity for each b-value and estimated D (output of Kalman filter), one hidden layer

with 15 nodes, and the output layer returned the amounts of f and D^* (Figure 1c).

Statistical analysis

A T-test was used to compare the proposed and conventional methods' estimated parameters with ground truth (actual values). Furthermore, the Pearson correlation test was performed to check the similarity between ground truth and calculated results.

Results

According to the results of the first experienced: 1) reduction of noise is possible in the light of using filters such as the Kalman filter, modifying the diffusion coefficient and reducing the effects of noise (Figure 2), i.e. the variance is reduced and 2) blood movement in the capillary network as a source of unwanted motion can be predicted and canceled by exploiting the Kalman filter. As seen in Figure 3, the Kalman filter not only reduced noise effects but also highly rejected blood movement artifacts. Therefore, D's bias decreased less than 1%.

The Kalman filter estimate of D was $0.0010\pm1.3\times10^{-5}$ (mean±standard deviation), while the conventional estimate was $0.0012\pm3.6\times10^{-5}$, where the actual D value was 0.0010 (mm^2/s). The T-tests results indicated that the estimation performance of the proposed method is significantly better than the conventional method (P-value<0.01). The results of the conventional method are associated with a bias due to the effect of ignoring the blood flow in the capillary network. On the other hand, the Kalman filter can consider the effects of microcirculation blood flow as inputs and lessens its impact on estimations. Comparing Kalman filter results and actual values using the T-test shows no significant alteration (P=0.25). However, the estimates of the conventional method are substantially different from ground-truth values and Kalman filter estimates (P<0.0001) (Table 1).

Finally, using Kalman filter output as an input for the second neural network improved the estimation of IVIM-outputs significantly.

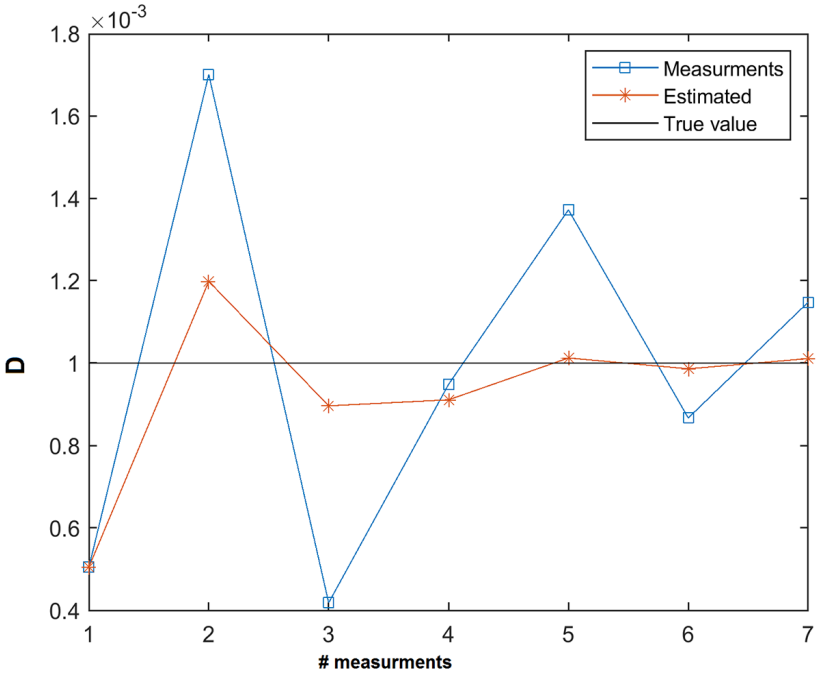

Figure 2: Measurements of diffusion coefficient (D) have been shown as blue color and vary because of noise, although; the Kalman filter improves the result and increases accuracy.

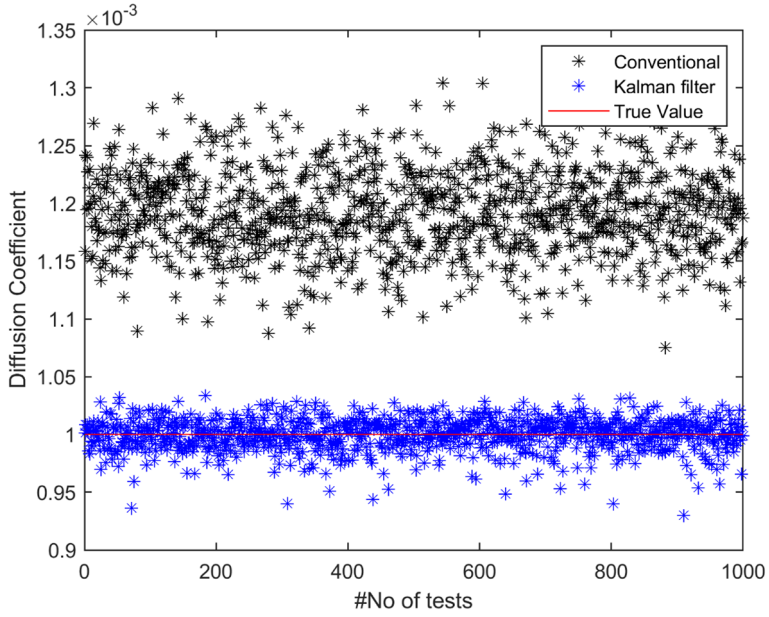

Figure 3: Comparison of results of Kalman-Filter and conventional method to calculate diffusion coefficient (D), as it can be seen *D* in the conventional method has a bias.

Table 1: Statistical comparison of Kalman filter and conventional method by T-Test. where h is the decision based on T-Test, 0 means that zero hypothesis is not rejected and 1 means that alternative hypothesis significantly is meaningful.

T-Test	h	*P*-value
Kalman Filter vs True values	0	0.2440
Conventional Method vs True values	1	1.8563e-48
Conventional Method vs Kalman filter	1	2.5404e-33

The bias of *f* and *D** reduced to about 4% and 12%, respectively (Figure 4 d-f). On the contrary, the results based on just neural networks are illustrated in Figure 4 a-c, i.e. estimating IVIM-outputs is not as accurate as of combining Kalman filter and neural networks. The bias of just neural networks for diffusion coefficient (*D*) is about 11%, that of blood fraction (*f*) is around about 8%, and this amount is in the range of 16% for pseudodiffusion *D**, which are higher than their counterparts mentioned above.

Discussion

The IVIM model is widely used and considered as a promising method due to benefit of both functional and structural information in the form of perfusion and diffusion images, without any need to contrast agent injection. Furthermore, this is a noninvasive method compared to conventional perfusion MR imaging such as dynamic contrast- enhanced (DCE) and dynamic susceptibility contrast-enhanced (DSC), enriched by diffusion information simultaneously [3]. After considering these advantages, because of the nonlinear behavior of the IVIM model and noise, IVIM output must be calculated carefully.

IVIM has three outputs: diffusion (*D*), blood fraction (*f*) and pseudo-perfusion (*D**) that *D* is more robust than *f* and *D**. Perfusion-related parameters are vulnerable to contamination by noise. Some studies have proposed different methods to increase the accuracy of these outputs [18, 26]. Novel techniques such as neural networks showed a good performance in estimating IVIM outputs [27].

Other methods such as Bayesian and non-

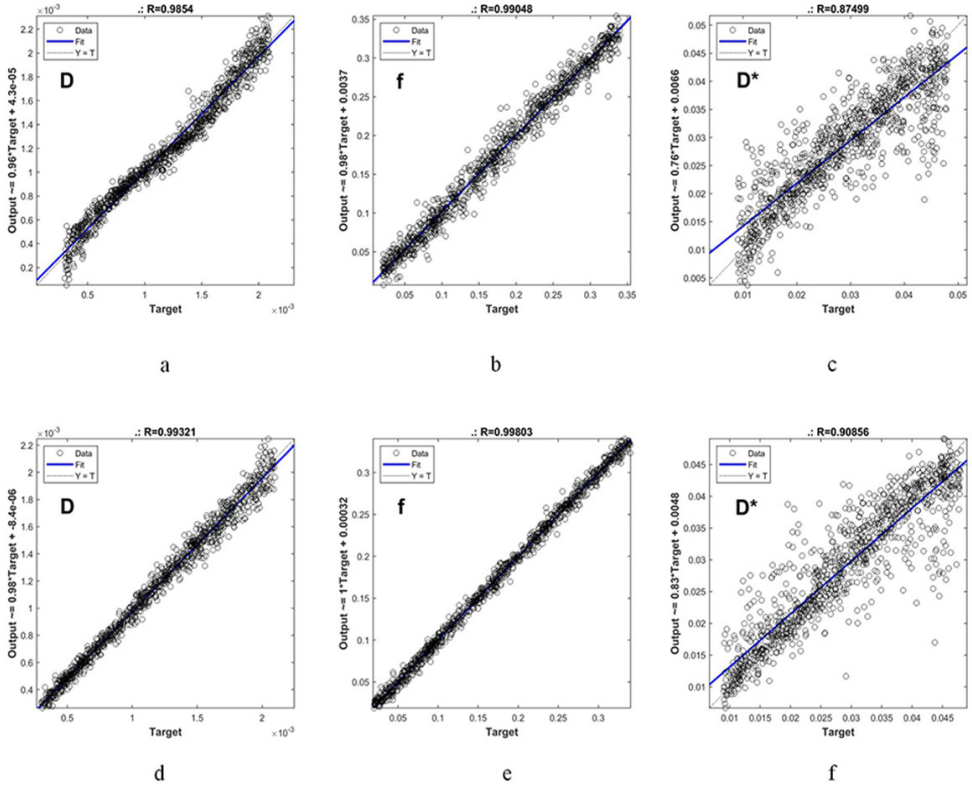

Figure 4: Comparison of using neural networks by itself and neural networks in combination with Kalman filter is depicted as; **a**) **b**) **c**) represent results of diffusion coefficient (*D*), fraction of blood (*f*) and pseudodiffusion coefficient (*D**) when just the neural network is applied. **d**) represents the result of Kalman filter **e**) **f**) represent *f* and *D** as the results of the neural network when estimated *D* is used as the input in the network.

linear solutions need some defined distributions and initial parameters that might mislead the outputs and sometimes their effects are recognizable in approaching boundaries and initial values [28]. Since neural networks do not need this kind of initialization and evolve their model just based on input data, it improves the IVIM output accuracy and confirms that its output is reliable and reproducible. Advantages of neural networks compared with other solutions consists of 1) no need to initialize, 2) no approaching boundary condition, 3) no need to define a distribution for parameters, and 4) with the robust system in the presence of noise. Therefore, training is a crucial factor for the neural network.

Observation is considered as a way to improve the estimation power of neural networks and purified diffusion coefficient is added to the input layer in the proposed method. Since the Kalman filter purifies the diffusion coefficient, using estimated *D* as a new input increases the accuracy of perfusion parameters (*f* and *D**).

A bias is in *D*'s estimates of other methods because of disregarding perfusion signal decay in higher b-values. Kalman filter considers perfusion factors and increases the accuracy of the *D*'s estimates successfully. Statistical tests reveal that the proposed-method estimations outperformed the conventional method. The conventional approach results in a bias in DWI estimations that eliminate micro-vessel blood circulation displacements. However, consider-

ing the impacts of microcirculation blood flow as input, the Kalman filter reduces its effects on estimates. Finally, a combination of Kalman filter and neural networks is applied. The final results endorse that the proposed method improves the validity of results successfully.

Conclusion

The Kalman filter along with the neural network increases the accuracy and validity of the IVIM model. Although the IVIM model benefits from both functional and structural information, the lack of validity in the low SNR regime delimits its application in clinical settings. The Kalman filter also improves the quality of IVIM images, resulting in increasing the accuracy of perfusion parameters. Finally, the results caused the reliability of the IVIM model, improving diagnostic accuracy in a fast and non-invasive way.

Acknowledgment

This research has been supported by Tehran University of Medical Sciences; grant number 36937.

Authors' Contribution

All authors contributed to the study's conception and design. S. Sharifzadeh Javidi performed data collection and analysis. The first draft of the manuscript was written by S. Sharifzadeh Javidi. R. Ahadi and H. Salighehrad commented on previous versions of the manuscript. All authors read and approved the final manuscript.

Ethical Approval

The research was approved by the Institutional Ethical Committee of Tehran University of Medical Sciences (Approval code: IR.TUMS.MEDICINE.REC.1396.4257).

Informed consent

All experimental procedures were conducted according to The Declaration of Helsinki; written informed consent was obtained from participants.

Conflict of Interest

None

References

1. Basser PJ. Inferring microstructural features and the physiological state of tissues from diffusion-weighted images. *NMR Biomed*. 1995;**8**(7-8):333-44. doi: 10.1002/nbm.1940080707. PubMed PMID: 8739270.
2. Le Bihan D, Breton E, Lallemand D, Grenier P, Cabanis E, Laval-Jeantet M. MR imaging of intravoxel incoherent motions: application to diffusion and perfusion in neurologic disorders. *Radiology*. 1986;**161**(2):401-7. doi: 10.1148/radiology.161.2.3763909. PubMed PMID: 3763909.
3. Le Bihan D. What can we see with IVIM MRI? *Neuroimage*. 2019;**187**:56-67. doi: 10.1016/j.neuroimage.2017.12.062. PubMed PMID: 29277647.
4. Bley TA, Wieben O, Uhl M. Diffusion-weighted MR imaging in musculoskeletal radiology: applications in trauma, tumors, and inflammation. *Magn Reson Imaging Clin N Am.* 2009;**17**(2):263-75. doi: 10.1016/j.mric.2009.01.005. PubMed PMID: 19406358.
5. Ni X, Wang W, Li X, Li Y, Chen J, Shi D, et al. Utility of Diffusion-Weighted Imaging for Guiding Clinical Management of Patients With Kidney Transplant: A Prospective Study. *J Magn Reson Imaging*. 2020;**52**(2):565-74. doi: 10.1002/jmri.27071. PubMed PMID: 32030832.
6. Huang HM. Reliable estimation of brain intravoxel incoherent motion parameters using denoised diffusion-weighted MRI. *NMR Biomed.* 2020;**33**(4):e4249. doi: 10.1002/nbm.4249. PubMed PMID: 31922646.
7. Cheng ZY, Feng YZ, Hu JJ, Lin QT, Li W, Qian L, et al. Intravoxel incoherent motion imaging of the kidney: The application in patients with hyperuricemia. *J Magn Reson Imaging.* 2020;**51**(3):833-40. doi: 10.1002/jmri.26861. PubMed PMID: 31318112.
8. Beyhan M, Sade R, Koc E, Adanur S, Kantarci M. The evaluation of prostate lesions with IVIM DWI and MR perfusion parameters at 3T MRI. *Radiol Med*. 2019;**124**(2):87-93. doi: 10.1007/s11547-018-0930-3. PubMed PMID: 30276599.

9. Surer E, Rossi C, Becker AS, Finkenstaedt T, Wurnig MC, Valavanis A, et al. Cardiac-gated intravoxel incoherent motion diffusion-weighted magnetic resonance imaging for the investigation of intracranial cerebrospinal fluid dynamics in the lateral ventricle: a feasibility study. *Neuroradiology.* 2018;**60**(4):413-9. doi: 10.1007/s00234-018-1995-3. PubMed PMID: 29470603.
10. Stejskal EO, Tanner JE. Spin Diffusion Measurements: Spin Echoes in the Presence of a Time Dependent Field Gradient. *The Journal of Chemical Physics*. 1965;**42**(1):288-92. doi: 10.1063/1.1695690.
11. Le Bihan D, Turner R, Douek P, Patronas N. Diffusion MR imaging: clinical applications. *AJR Am J Roentgenol.* 1992;**159**(3):591-9. doi: 10.2214/ajr.159.3.1503032. PubMed PMID: 1503032.
12. Turner R, Le Bihan D, Maier J, Vavrek R, Hedges LK, Pekar J. Echo-planar imaging of intravoxel incoherent motion. *Radiology.* 1990;**177**(2):407-14. doi: 10.1148/radiology.177.2.2217777. PubMed PMID: 2217777.
13. Padhani AR, Liu G, Koh DM, Chenevert TL, Thoeny HC, Takahara T, et al. Diffusion-weighted magnetic resonance imaging as a cancer biomarker: consensus and recommendations. *Neoplasia*. 2009;**11**(2):102-25. doi: 10.1593/neo.81328. PubMed PMID: 19186405. PubMed PMCID: PMC2631136.
14. Hashim E, Yuen DA, Kirpalani A. Reduced Flow in Delayed Graft Function as Assessed by IVIM Is Associated With Time to Recovery Following Kidney Transplantation. *J Magn Reson Imaging.* 2021;**53**(1):108-17. doi: 10.1002/jmri.27245. PubMed PMID: 32602206.
15. Lévy S, Rapacchi S, Massire A, Troalen T, Feiweier T, Guye M, et al. Intravoxel Incoherent Motion at 7 Tesla to quantify human spinal cord perfusion: Limitations and promises. *Magn Reson Med.* 2020;**84**(3):1198-1217. doi: 10.1002/mrm.28195. PubMed PMID: 32057128.
16. Federau C, Hagmann P, Maeder P, Muller M, Meuli R, Stuber M, et al. Dependence of brain intravoxel incoherent motion perfusion parameters on the cardiac cycle. *PLoS One.* 2013;**8**(8):e72856. doi: 10.1371/journal.pone.0072856. PubMed PMID: 24023649. PubMed PMCID: PMC3758329.
17. Karchevsky M, Babb JS, Schweitzer ME. Can diffusion-weighted imaging be used to differentiate benign from pathologic fractures? A meta-analysis. *Skeletal Radiol*. 2008;**37**(9):791-5. doi: 10.1007/s00256-008-0503-y. PubMed PMID: 18551290.
18. Cho GY, Moy L, Zhang JL, Baete S, Lattanzi R, Moccaldi M, et al. Comparison of fitting methods and b-value sampling strategies for intravoxel incoherent motion in breast cancer. *Magn Reson Med.* 2015;**74**(4):1077-85. doi: 10.1002/mrm.25484. PubMed PMID: 25302780. PubMed PMCID: PMC4439397.
19. Ye C, Xu D, Qin Y, Wang L, Wang R, Li W, et al. Estimation of intravoxel incoherent motion parameters using low b-values. *PLoS One.* 2019;**14**(2):e0211911. doi: 10.1371/journal.pone.0211911. PubMed PMID: 30726298. PubMed PMCID: PMC6364995.
20. While PT. A comparative simulation study of bayesian fitting approaches to intravoxel incoherent motion modeling in diffusion weighted MRI. *Magn Reson Med*. 2017;**78**(6):2373-87. doi: 10.1002/mrm.26598. PubMed PMID: 28370232.
21. Iima M, Yano K, Kataoka M, Umehana M, Murata K, Kanao S, et al. Quantitative non-Gaussian diffusion and intravoxel incoherent motion magnetic resonance imaging: differentiation of malignant and benign breast lesions. *Invest Radiol.* 2015;**50**(4):205-11. doi: 10.1097/RLI.0000000000000094. PubMed PMID: 25260092.
22. Javidi SS, Rad HS. Using Kalman Filter to Improve the Accuracy of Diffusion Coefficients in MR Imaging: A Simulation Study. *Iranian Journal of Radiology*. 2019;**16**(Special Issue). doi: 10.5812/iranjradiol.99153.
23. Le Bihan D, Breton E, Lallemand D, Aubin ML, Vignaud J, Laval-Jeantet M. Separation of diffusion and perfusion in intravoxel incoherent motion MR imaging. *Radiology.* 1988;**168**(2):497-505. doi: 10.1148/radiology.168.2.3393671. PubMed PMID: 3393671.
24. Kalman RE. Contributions to the theory of optimal control. *Bol Soc Mat Mexicana*. 1960;**5**(2):102-19.
25. Weill LR, De Land PN. The Kalman filter: an introduction to the mathematics of linear least mean square recursive estimation. *International Journal of Mathematical Education in Science and Technology*. 1986;**17**(3):347-66. doi: 10.1080/0020739860170311.
26. Fusco R, Sansone M, Petrillo A. A comparison of fitting algorithms for diffusion-weighted MRI

data analysis using an intravoxel incoherent motion model. *Magma.* 2017;**30**(2):113-20. doi: 10.1007/s10334-016-0591-y. PubMed PMID: 27670762.

27. Bertleff M, Domsch S, Weingärtner S, Zapp J, O'Brien K, Barth M, et al. Diffusion parameter mapping with the combined intravoxel incoherent motion and kurtosis model using artificial neural networks at 3 T. *NMR Biomed*. 2017;**30**(12):e3833. doi: 10.1002/nbm.3833. PubMed PMID: 28960549.
28. Jalnefjord O, Andersson M, Montelius M, Starck G, Elf AK, Johanson V, et al. Comparison of methods for estimation of the intravoxel incoherent motion (IVIM) diffusion coefficient (D) and perfusion fraction (f). *Magma*. 2018;**31**(6):715-23. doi: 10.1007/s10334-018-0697-5. PubMed PMID: 30116979.